Influence the loading conditions and the stress concentrators on the spatial-time inhomogeneity due to the yield delay and the jerky flow: study by using the digital image correlation and the infrared analysis

Tatyana V. Tretyakova*, Valery E. Wildemann
Center of Experimental Mechanics, Perm National Research Polytechnic University, 29 Komsomolsky prospekt, Perm 614990, Russia
cem.tretyakova@gmail.com, wildemann@pstu.ru

ABSTRACT. The paper deals with the investigation of the temporal instabilities and spatial localization due to the Lüders behavior and the Portevin–Le Chatelier effect in the carbon steel C1010 and the aluminum-magnesium alloy AA5052, which manifest the unstable plastic flow. The digital image correlation technique and the infrared thermography were used to capture and study the processes of the initiation and propagation of the deformation bands. The main part of the research focuses on the estimation of the influence of the loading system's stiffness on the irregular plastic flow, which was carried out on flat specimens with complicated geometry and on specimens with additional deformable parts.

KEYWORDS. Plasticity; Experimental strain analysis; Stress concentrator; Digital image correlation; Infrared analysis.

Citation: Tretyakova, T. V., Wildemann, V. E., Influence the loading conditions and the stress concentrators on the spatial-time inhomogeneity due to the yield delay and the jerky flow: study by using the digital image correlation and the infrared analysis, Frattura ed Integrità Strutturale, 42 (2017) 303-314.

Received: 09.03.2017
Accepted: 18.08.2017
Published: 01.10.2017

INTRODUCTION

The experimental study of the mechanical behavior of the structural materials and the spatial-time inhomogeneity of plastic deformation is an important subject in mechanics of deformable solids. In uniaxial tension tests, some metals and alloys exhibit irregular plastic flow. At the stage of the yield delay the unstable flow results in inhomogeneous deformation due to the Chernov-Lüders behavior. On the surface of a specimen during the yield point and the yield plateau forming the deformation bands of localized plastic flow initiate and propagate along the gauge length. A.H. Cottrell put forward the theoretical description of the upper/lower stress, in which case the yield point on the stress-strain curve explained by dislocation theory at the microscopic level.

It is well known, that aluminum-magnesium alloy manifests the Savart-Masson effect in conditions of the strength loading ($\dot{\varepsilon}_0 = const$) or the Portevin-Le Chatelier effect in conditions of the kinematic loading ($\dot{\sigma}_0 = const$) in a given range of temperature and strain/stress rate [1-3]. The jerky flow results in the numerous drops on the load diagrams and

inhomogeneous strain fields with different types of deformation bands (A, B, or C) [4]. Despite the considerable investigations that have been conducted on the effects of the inelastic deformation and the irregular plastic flow, the yield delay effect and the PLC effect is still debated. Some research deals with the influence of specimen geometry [5, 6] and chemical composition [4], other research estimates the influence of loading conditions and external test parameters on the PLC effect [7-10] and the Lüders behavior [11, 12].
Advanced materials testing equipment and high-accuracy measuring systems make it possible to represent complicated loading conditions, which are close to operation conditions. When studying the plastic strain inhomogeneity, it is expedient to use optical methods, such as photoelastic technique, speckle pattern interferometry, digital image correlation technique (DIC), and infrared (IR) thermography as well [2, 6, 12].
The purpose of the present study is to detect and analyze the spatiotemporal characteristics of the Lüders behavior and the PLC effect with considering the loading system's stiffness and the stress concentrators. The DIC-technique and IR-analysis were applied to observe the evolution of the inhomogeneous strain and temperature fields, and to study the morphology and kinetics of the deformation bands in metals during uniaxial tension tests. The irregularity of the plastic flow was correlated with the associated serrations observed on the stress-strain diagrams. The initiation and propagation of the Lüders and the PLC bands were carried out on specimens with complicated geometry.

EXPERIMENTAL PROCEDURE

Material

The materials studied in this research is the carbon steel C1010 and the aluminum-magnesium alloy AA5052. The chemical compositions are given below in Table 1 and Table 2. The flat specimens were made by water jet cutting from thick rolled sheets with a thickness of 3 mm. Specimens were tested in the state as received without the heat treatment process. For the carbon steel the average grain size was 27 μm (Fig. 1). The phase analysis revealed that the proportion of the ferrite in the steel as a structural component was 70 %, and the perlite – 30 %.

Fe	C	Si	Mn	Cr	Ni	Cu
99.0	0.18	0.20	0.35	0.04	0.03	0.04

Table 1: The chemical composition (weight percent) of the carbon steel.

Figure 1: The microstructure of the carbon steel C1010.

Al	Mg	Mn	Fe	Si	Others
95.2	3.18	0.38	0.27	0.8	0.17

Table 2: The chemical composition (weight percent) of the Al-Mg alloy.

Testing procedure

The mechanical tests in the paper were carried out in the Instron 8850 servo-hydraulic biaxial testing system (100 kN/1000 N·m, 30 Hz) and the Instron 5989 electromechanical testing system (600 kN) at room temperature. The 3-D digital image correlation measurement system Vic-3D was used to observe and characterize the inhomogeneous strain fields due to the Lüders and PLC bands. The Vic-3D was used with the set of two high-resolution cameras (Prosilica, 16 Mp) and the set of the high-speed cameras (Gazelle, 4 Mp). The software of the system is based on the digital image correlation technique. The DIC is a highly effective computer-vision-based technique, which provides estimation of the displacement and strain fields on specimen surface by matching the reference subsets in the undeformed image (before loading) with the target subsets in the deformed images (captured during test). The surface of all specimens was painted with finely sprayed white and black dots to increase the image contrast. The thermographic analysis was used to estimate the temperature fields, that is, the infrared camera Flir SC7700 with a resolution of 640×512 pixels was applied. It is important to notice that the software and hardware synchronization of the testing and measurement equipment was carried out with the DAQ device NI USB-6251. Fig. 2 shows the testing and measuring equipment used in the research.

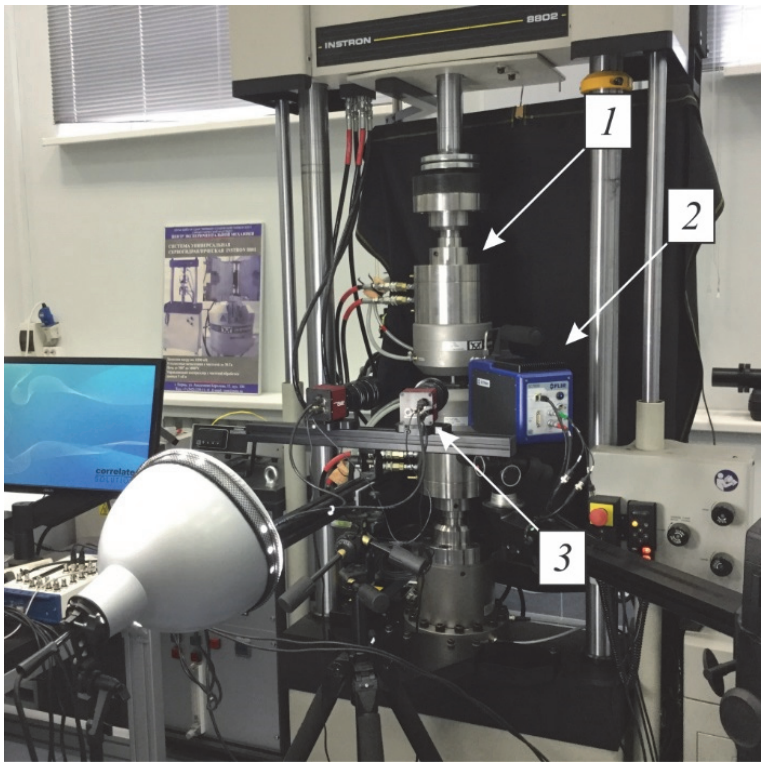

Figure 2: The Instron 8850 servo-hydraulic biaxial test system (*1*) with registration of the strain and temperature fields by using the infrared camera Flir SC7700 (*2*) and the 3D-digital image correlation measurement system Vic-3D (*3*).

As written above, the aim of this study is to estimate the influence of the stress concentrators and the stiffness of the loading system (R_{LS}) on the effects of the serrated flow, on the initiation of strain bands of localized plastic deformation. So, three groups of specimens are used in this investigation. The first group includes the standard flat dog-bone specimens, which have a width of 12 and 20 mm; a gauge length of 50, 75 and 100 mm; a thickness of 2 and 3 mm. The second group is a set of flat specimens with stress concentrators: a single center hole with a diameter of 3 and 6 mm (see Fig. 3 (a)); two holes with a diameter of 3 mm (Fig. 3 (b)). Finally, the flat specimens with an additional deformable part

(Fig. 3 (c)) and the original specimens with complicated geometry (Fig. 3 (d)) were carried out in order to estimate the stiffness of the loading system. We can manage (decrease) the stiffness (R_{LS}) by changing the width (b_c) and the length (l_c) of the additional deformable part of specimens (Fig. 3 (c)). The shape of the specimen with complicated geometry is to be describe in more detail. As shown in Fig. 3 (d), there are two 'L-shaped' holes with a length of L_0 in the central part of the specimen, which create the system of the gauge (*1*) and control (*2*) sections; and two rectangular parts (*3*, *4*) on the left/right. Note that during loading, the peripheral parts *3* and *4* deform together with the central part; and increase the stiffness of the loading system (R_{LS}) relatively to the gauge length of the specimen. The dimensioning specifications of the specimens with complicated geometry will be shown below. The research program includes uniaxial tension tests on flat specimens with a constant strain rate ranging from 0.33×10^{-4} s^{-1} to 0.33×10^{-2} s^{-1}.

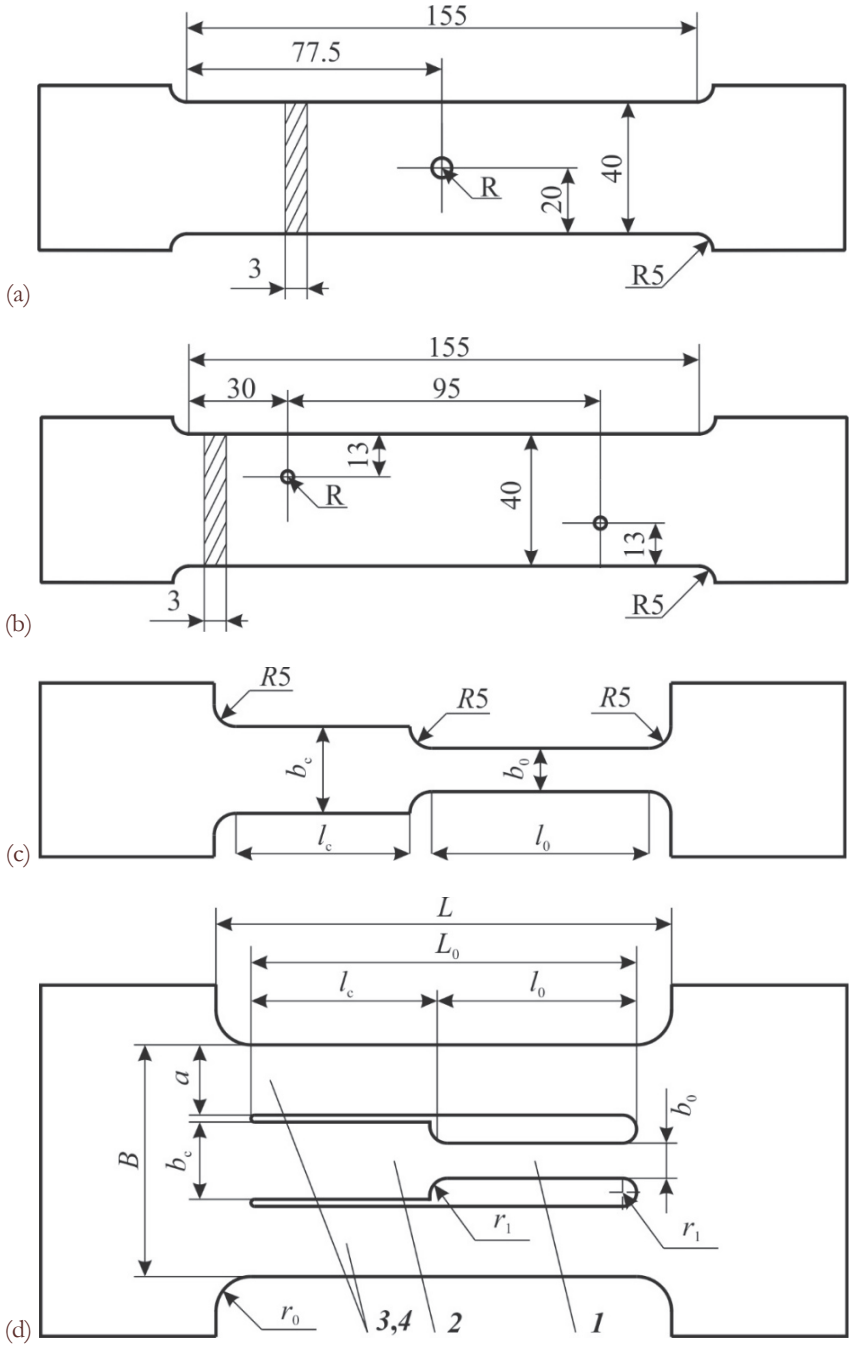

Figure 3: Sketches of flat specimens used in the investigation.

RESULTS AND DISCUSSIONS

Experimental strain fields analysis during the uniaxial tension of the flat dog-bone specimens

This section describes some results on experimental investigation of the spatial-time inhomogeneity due to the Chernov-Lüders behavior during uniaxial tension of flat dog-bone specimens. The longitudinal strain, the local strain rate and temperature fields were analyzed on the specimens' surfaces according with the stress-strain curves. Fig. 4 shows the 'σ–ε' curve and the evolution of local strain rate observed on the surface of the carbon steel specimen ($l_0 = 100$ mm, $b_0 = 20$ mm, $h_0 = 3$ mm), at the nominal strain rate of $1.67 \cdot 10^{-3}$ s^{-1}. It is important, that the stage of the yield drop and the yield plateau forming was under observation, that is, the time range was from t_1 to t_9 (see Fig. 4). At the initial stage the deformation of the material was running uniformly up to the upper yield point, or the yield drop. The initiation of the Chernov- Lüders band caused the rapid jump of the longitudinal strain level registered on the specimen surface from the grip side at moment of transition from the yield drop to the yield plateau, or the lower yield point. At the same time, the load value declined. When the strain band reached the opposite side of the specimen, the configuration of the longitudinal strain fields became almost homogeneous. It is important to note that in the region where the front of the localized strain had passed, the material's deformation processes stopped until the next deformation stage — the material hardening stage. More details can be found in [13].

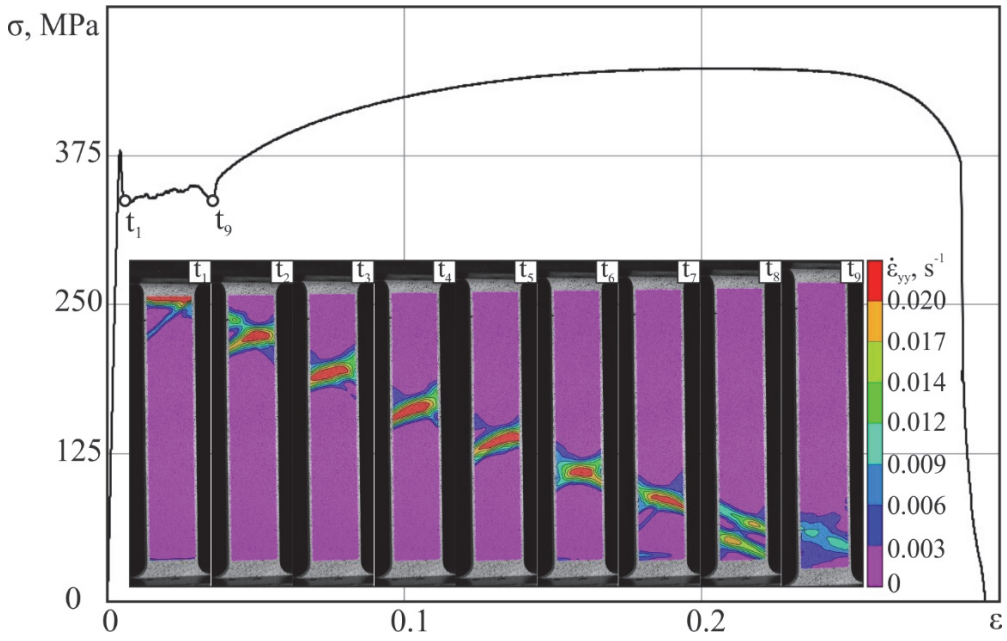

Figure 4: Evolution of local strain rate showing the propagation the Chernov-Lüders bands on the specimen surface during a tension test ($t = t_1 - t_9$).

The flat dog-bone specimens (Al-Mg alloy) with a width of 12 mm and 20 mm; a gauge length of 50, 75 and 100 mm were tested at the nominal strain rate of $1.67 \cdot 10^{-4}$ s^{-1}. Fig. 5 depicts the set of profiles calculated along the gauge length of the specimen with a width of 10 mm, a length 75 mm and a thickness of 3 mm based on the analysis of the strain fields. A time gap between profiles is constant and equals $\Delta t = 2.0$ s. The direction of the Chernov-Lüders band propagation is marked with the arrow (v_b). The average value of the longitudinal strain (ε_H) achieved after the strain band propagation (line *1*, Fig. 5) was around $\varepsilon_H = 1.26$ %.

To estimate the influence of the strain rate and specimen geometry (width, length) on the Chernov- Lüders behavior, mechanical tests were carried out with different crosshead velocities ranging from 0.5 mm/min to 10 mm/min. A brief summary of the mechanical tests carried out in the present study described in Table 3 and Table 4, where k_b — a

coefficient of the strain inhomogeneity. For specimens with the width of 12 mm the average value of the k_b is around 0.010, and for specimens with the width of 20 mm — $k_b = 0.011$.

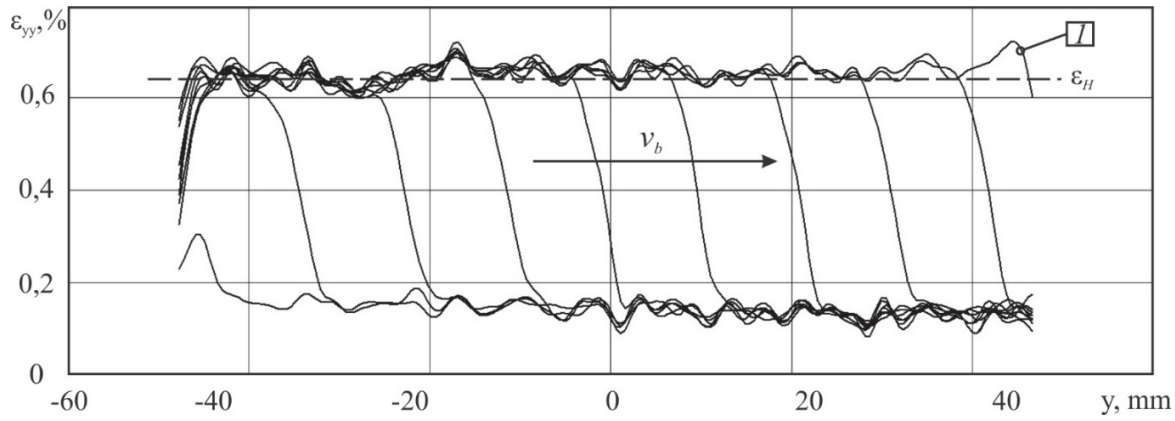

Figure 5: Profiles of the longitudinal strain (ε_{yy}), calculated along the flat specimen of Al-Mg alloy at the stage of the yield drop and yield plateau forming

$\dot{u}_0$, mm/min	v_b, mm/min	$k_b = \dot{u}_0 / v_b$	ε_H, %
0.5	55.2	0.009	1.29
1.0	104.6	0.010	1.20
1.0	97.6	0.010	1.17
5.0	458.5	0.011	1.28

Table 3: Influence of the crosshead velocity on the Chernov–Lüders band propagation ($b_0 = 12.0$ mm).

$\dot{u}_0$, mm/min	v_b, mm/min	$k_b = \dot{u}_0 / v_b$	ε_H, %
1.0	98.4	0.010	1.21
1.0	92.0	0.011	1.22
5.0	422.9	0.012	1.35
10.0	845.1	0.012	1.36

Table 4: Influence of the crosshead velocity on the Chernov–Lüder's band propagation ($b_0 = 20.0$ mm).

Profiles of the longitudinal strain were calculated along the longitudinal direction at the elastoplastic deformation stage and the stage of hardening as well. The numerical the Portevin-Le Chatelier bands were observed and characterize on the surfaces of the specimens during tension tests. Fig. 6 shows results for the specimen of Al-Mg alloy with a width of 20 mm and a length of 100 mm, note that the time gap Δt between profiles is 2 seconds. Lines *1–10* correspond to the moments of the relative levelling-off of the longitudinal strain on the specimen's surface. The experimental study of the strain fields during the uniaxial tension of specimens of the Al-Mg alloy revealed the quasi-periodic character of the development of plastic deformations under conditions of discontinuous yielding of the material, which included the alternation of the stages of initiation and propagation of the strain bands. These processes were characterized by a high degree of strain inhomogeneity and the existence of relative leveling-off of strain fields [14, 15].

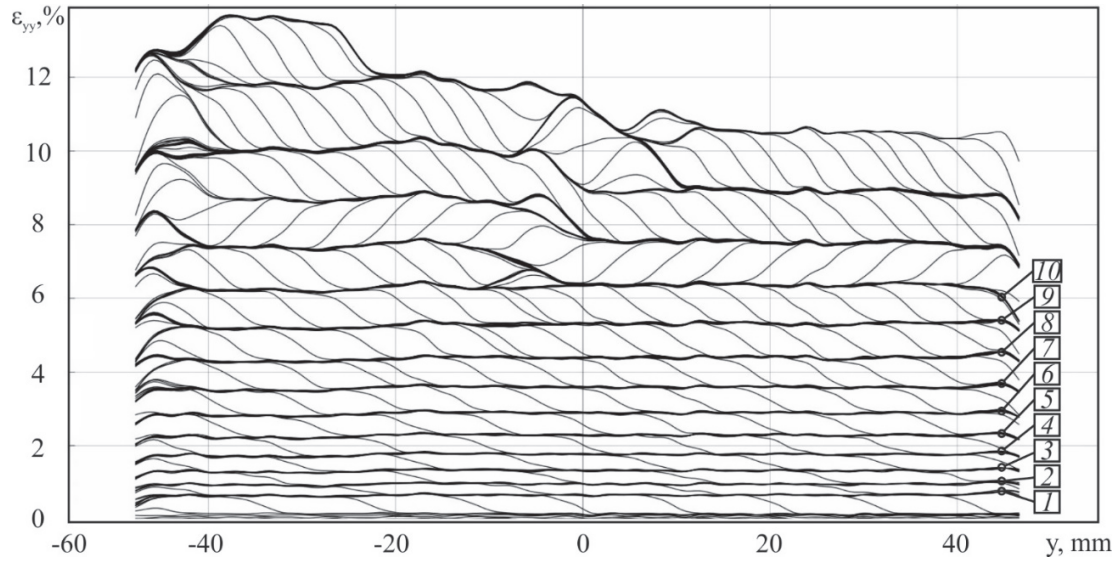

Figure 6: Set of the profiles of the longitudinal strain (ε_{yy}) showing the effect of the quasi-periodic character during the uniaxial tension test.

The influence of the stress concentrators

Fig. 7 presents the load-displacement curve obtained for uniaxial tension test on the flat specimen with stress concentrators (a pair holes with diameters of 3 mm), for a nominal strain-rate of $1.67 \cdot 10^{-3}$ s^{-1}. Fig. 8 shows the evolution of the inhomogeneous local strain rate and temperature fields. It is important to notice, that the loading curves include the stage of the yield plateau forming, despite the stress concentrators); also, the plastic flow localizes in the form of the strain bands on the specimen surface. When load increasing, the Chernov-Lüders bands passed lengthwise the specimen surface.

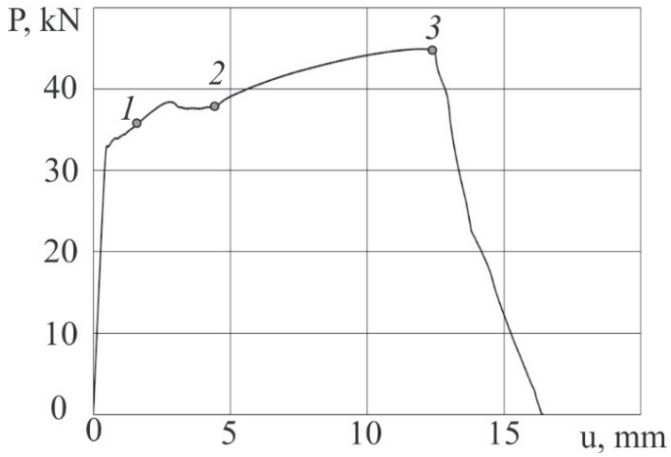

Figure 7: The load-displacement curve for uniaxial tension test on the flat specimen with two holes.

The influence of the loading system's stiffness

It is well known, that the interaction between a loading system and deformable solid bodies plays a key role in the transition from the stage of equilibrium damage accumulation to the non-equilibrium, or avalanche, stage of the material's failure. The original experimental methods, which provide managing of the loading system characteristics, were used for this study of the mechanical behavior and the patterns of the macroscopic localization of the plastic flow with taking into account the real properties of the loading conditions. The flat specimens (Al-Mg alloy) with additional deformable parts (see Fig. 3 (c)) and specimens with the complicated geometry (Fig. 3 (d)) were tested on the uniaxial tension with a constant nominal strain rate of $1.67 \cdot 10^{-3}$ s^{-1}.

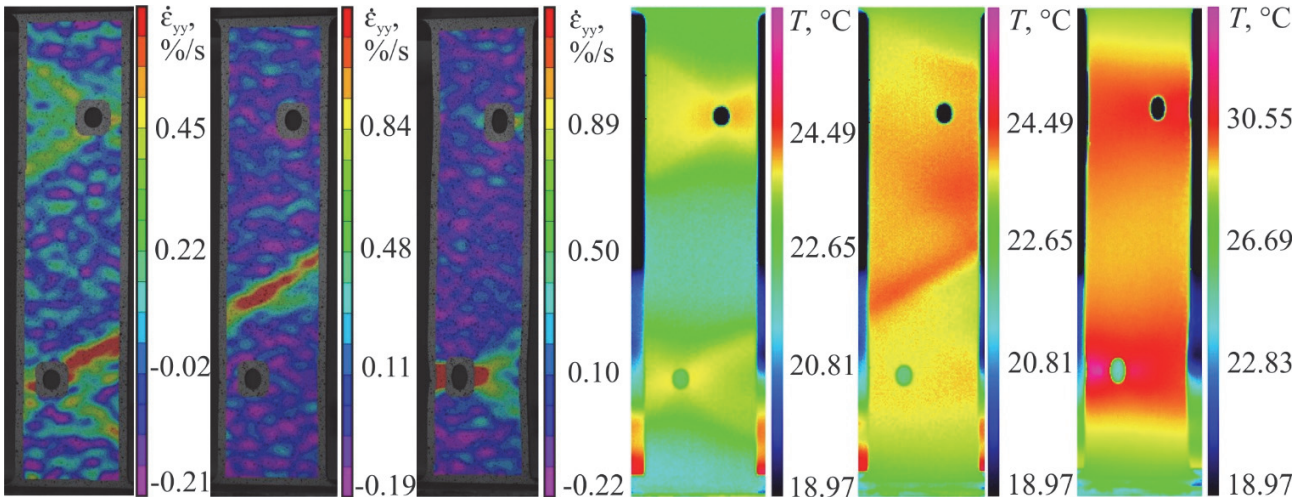

Figure 8: Evolution of the inhomogeneous local strain rate and temperature fields on the surface of the flat specimens with two holes.

The loading system is the set of deformable bodies, which deform due to the load transfer to the region under consideration. In tests the stiffness of the loading system (R_{LS}) includes the elements of a testing machine (a frame, grips, a crosshead, a load cell) and deformable parts of a specimen, and is defined as:

$$R_{LS} = \frac{R_c R_M}{R_c + R_M} \tag{1}$$

where $R_c = \frac{E h_0 b_c}{l_c}$ – is a stiffness of the additional deformable parts of a specimen (a control part), R_M – is a stiffness of a loading system, E – elasticity modulus of the material under study. The Instron 5989 has the stiffness of $R_M = 200$ MN/m at the load of $P = 2 \div 5$ kN. By managing the length of the additional deformable part, or the control part, we obtained the loading system stiffness in range of $R_{LS} = 55.8 \div 83.6$ MN/m.

The evolution of the inhomogeneous strain and temperature fields was analyzed, the patterns of the initiation and propagation of the Chernov-Lüder's and the Portevin-Le Chatelier bands were registered and studied as well. The control part stay in the elastic state throughout the loading (Fig. 9). Analysis of the set of the $\varepsilon_{yy} \sim y$ profiles and the coefficient of the inhomogeneity of the plastic deformation showed that the loading system (in the investigated range of the stiffness) had no effect on the irregularity of the plastic flow. Furthermore, the effect of the quasi-periodic homogenization of the plastic strain observed during uniaxial tension tests in conditions of the jerky flow manifestation.

The specimen with the complicated geometry as shown in Fig. 3 (d) has two 'L-shaped' crosscutting notches, which make the tie in the central area, consisting of two-tandem the gauge part *1* and the control part *2*, and two peripheral parts *3* and *4*. The parameters of the specimens with complicated configuration are shown in Table 5.

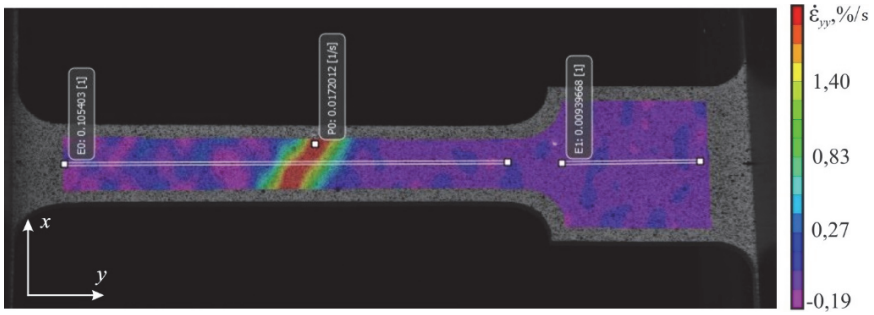

Figure 9: Inhomogeneous local strain rate fields on the surface of the flat specimen with additional deformable part.

Specimen	l_c	b_c	l_0	b_0	a	B	r_0
1	13.5	22	56.5	10	10	46	10
2	13.5	22	56.5	10	20	66	10
3	13.5	22	56.5	10	37	100	-
4	28.5	22	56.5	10	10	46	10
5	28.5	22	56.5	10	20	66	10
6	28.5	22	56.5	10	37	100	-
7	53.5	22	56.5	10	10	46	10
8	53.5	22	56.5	10	20	66	10
9	53.5	22	56.5	10	37	100	-

Table 5: The parameters of the specimens with complicated configuration.

The stiffness of the gauge part *1* is equal $R_0 = 42.5$ MN/m and defined as:

$$R_0 = \frac{Eb_0b_0}{l_0} \tag{2}$$

It follows thence, that the stiffness of the loading system can be defined as:

$$R_{LS} = b_0\left\{\frac{l_c}{Eb_c} + \left[\frac{2Ea}{l_0 + l_c} + \left(\frac{L_0 - L}{EB} + \frac{b_0}{R_M}\right)^{-1}\right]^{-1}\right\}^{-1} \tag{3}$$

Table 6 depicts a brief summary of the uniaxial tension tests for the stiffness of the loading system ranging from 58.3 to 177.9 MN/m.

No. specimen	R_{LS}, MN/m	No. specimen	R_{LS}, MN/m	No. specimen	R_{LS}, MN/m
1	103.7	4	79.8	7	58.3
2	136.5	5	94.7	8	64.5
3	177.9	6	113.0	9	71.5

Table 6: The obtained stiffness of the loading system for the specimens with complicated geometry.

Fig. 10 shows load-displacement curves obtained for uniaxial tension tests (a nominal strain-rate of $1.67 \cdot 10^{-3}$ s^{-1}) on the flat specimens with different widths of the peripheral parts: *1* – $a = 37$ mm, *2* – $a = 20$ mm, *3* – $a = 10$ mm, the length of the control part is 13.5 mm. As can be seen from Fig. 10 (a), the '*P-u*' curves exhibit the stage of the yield plateau forming and the jerky flow due to the Portevin-Le Chatelier. The stiffness of the loading system influences on the amplitude of the load serrations, that is, the increase of the stiffness causes the increase of 'tooth' amplitude.
On the surface of the specimens with complicated geometry, the man parts. Fig. 7 presents profiles of the longitudinal strain calculated along the gauge length for the gauge part (a line *1*) and peripheral parts (lines *2*, *3*). Note, that the $\varepsilon_{yy} \sim y$ profiles are symmetric for the left and right peripheral parts.

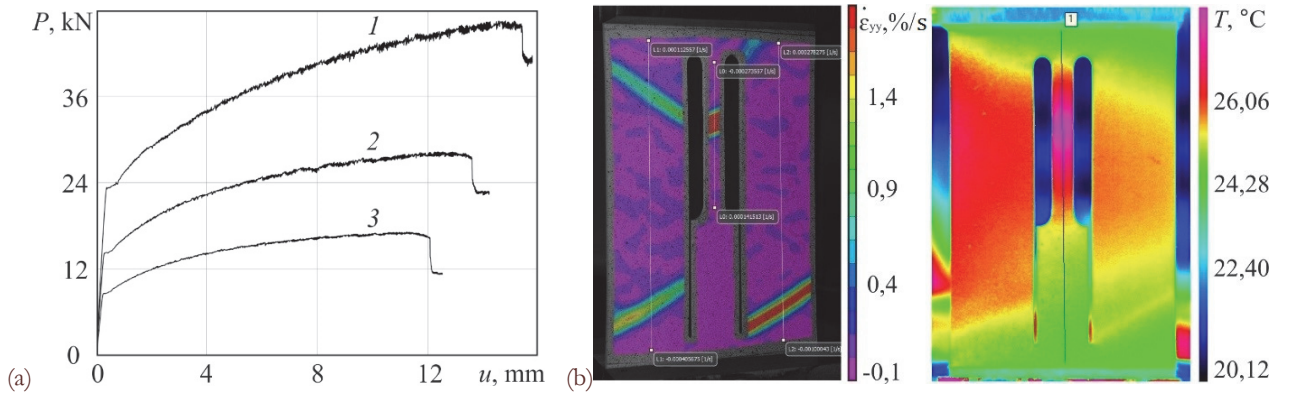

Figure 10: The load-displacement curves (a) and inhomogeneous local strain rate and temperature fields (b) for the specimen with $l_c = 13.5$ mm (*1* – $a = 37$ mm, *2* – $a = 20$ mm, *3* – $a = 10$ mm).

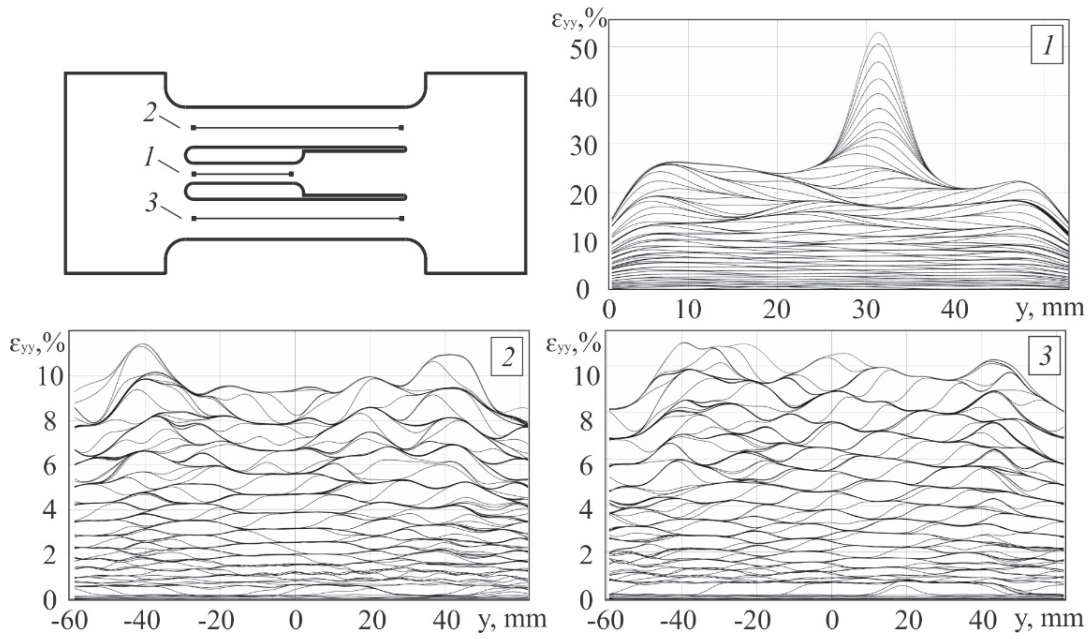

Figure 11: Set of the profiles of the longitudinal strain (ε_{yy}), drew along the gauge part (*1*) and the peripheral parts (*2*, *3*) of the specimen with complicated geometry during the uniaxial tension test

Conclusion

Complex experimental investigation of the temporal instabilities and the spatial localization due to the Lüders behavior, the Portevin–Le Chatelier effect and the shoulder or necking effect of aluminum-magnesium alloy and carbon steel was carried out on the base of combined use of the advanced test equipment, high-effect measuring systems and high-accuracy facilities. The results provide an important database for the development of the theoretical and numerical description of the material behavior in conditions of the serrated flow appearance, especially of the mechanisms and regularities of the Lüders and PLC bands nucleation and propagation.

ACKNOWLEDGEMENTS

This study was funded by the Russian Science Foundation (grant number 16-19-00069). The work was carried out in the Perm National Research Polytechnic University.

REFERENCES

[1] Benallal, A., Berstad, T., Børvik, T., Hopperstad, O.S., Koutiri, I., Nogueira de Codesa, R., An experimental and numerical investigation of the behavior of AA5083 aluminium alloy in presence of the Portevin–Le Chatelier effect, International Journal of Plasticity, 24 (2008) 1916–1945. DOI: 10.1016/j.ijplas.2008.03.008.

[2] Bernard, C., Coër, J., Laurent, H., Chauvelon, P., Relationship between local strain jumps and temperature bursts due to the Portevin-Le Chatelier effect in an Al-Mg Alloy, Experimental Mechanics, 53 (2013) 1025–1032. DOI: 10.1007/s11340-012-9711-4.

[3] Daghfas, O., Znaidi, A., Ben Mohamed, A., Nasri, R., Experimental and numerical study on mechanical properties of aluminum alloy under uniaxial tensile test, Frattura ed Integrità Strutturale, 39 (2017) 263-273. DOI: 10.3221/IGF-ESIS.39.24.

[4] Yilmaz, A., The Portevin-Le Chatelier effect: a review of experimental findings, Sci. Technol. Adv. Mater, 12 (2011) 1–16. DOI: 10.1088/1468-6996/12/6/063001.

[5] Aguirre, F., Kyriakides, S., Yun, H.D., Bending of steel tubes with Lüders bands, International Journal of Plasticity, 20 (2004) 1199–1225. DOI: 10.1016/j.ijplas.2003.05.001.

[6] de Codes, R.N., Benallal, A., Influence of specimen geometry on the Portevin-Le Châtelier effect due to dynamic strain aging for the AA5083-H116 aluminum alloy, Journal of Mechanics of Materials and Structures, 6 (2012) 951–968. DOI: 10.2140/jomms.2011.6.951.

[7] Benallal, A., Berstad, T., Børvik, T., Hopperstad, O.S., Nogueira de Codesa, R., Effects of strain rate on the characteristics of PLC deformation bands for AA5083-H116 aluminium alloy, Philosophical Magazine, 88 (2008) 3311-3338. DOI: 10.1080/14786430802468223.

[8] Xiaobo, Y., Fatigue crack growth of alumina alloy 7075-T651 under non proportional mixed mode I and mode II loads, Frattura ed Integrità Strutturale, 38 (2016) 148–154. DOI: 10.3221/IGF-ESIS.38.20.

[9] Zhang, J., Jiang, Y., An experimental study of inhomogeneous cyclic plastic deformation of 1045 steel under multiaxial cyclic loading, International Journal of Plasticity, 21 (2005) 2174–2190. DOI: 10.1016/j.ijplas.2005.02.003.

[10] Ozgowicz, W., Grzegorczyk, B., Pawelek, A., Wajda, W., Skuza, W., Piatkowski, A., Ranachowski, Z., Relation between the plastic instability and fracture of tensile tested Cu-Sn alloys investigated with the application of acoustic emission technique, Frattura ed Integrità Strutturale, 35 (2016) 11–20. DOI: 10.3221/IGF-ESIS.35.02.

[11] Tretiakova, T.V., Vildeman, V.E., Relay-race deformation mechanism during uniaxial tension of cylindrical samples of carbon steel: using digital image correlation technique, Frattura ed Integrità Strutturale, 24 (2013) 1–6. DOI: 10.3221/IGF-ESIS.24.01.

[12] Avril, S., Pierron, F., Sutton, M.A., Yan, J., Identification of elasto-visco-plastic parameters and characterization of Lüders behavior using digital image correlation and the virtual fields method, Mechanics of Materials, 40 (2008) 729–742. DOI: 10.1016/j.mechmat.2008.03.007.

[13] Vildeman, V. E., Lomakin, E. V., Tretiakova, T. V., Yield delay and space-time inhomogeneity of plastic deformation of carbon steel, Mechanics of Solids, 50 (2015) 412–420. DOI: 10.3103/S002565441504007X.

[14] Tretyakova, T.V., Wildemann, V.E., Study of spatial-time inhomogeneity of serrated plastic flow Al-Mg alloy: using DIC-technique, Frattura ed Integrità Strutturale, 27 (2014) 83–97. DOI: 10.3221/IGF-ESIS.27.10.

[15] Lomakin, E. V., Tretyakova, T. V., Wildemann, V. E., Effect of quasi-periodic homogenization of plastic deformations in the process of tension of samples of an aluminum–magnesium alloy, Doklady Physics, 60 (2015) 131–134. DOI: 10.1134/S1028335815030040.

NOMENCLATURE

σ	stress

ε	strain
$\dot{\varepsilon}_0$	strain rate
ε_{yy}	longitudinal strain
$\dot{\varepsilon}_{yy}$	rate of the local longitudinal deformation (along the Y-axis)
ε_b	value of the longitudinal strain achieved after the strain band propagation
y	coordinate of a point (along a specimen)
b_0	specimen width
l_0	gauge length of a specimen
h_0	specimen thickness
b_c	width of the additional deformable part of a specimen (the control part)
l_c	length of the additional deformable part of a specimen (the control part)
B	total width of the specimen with complicated geometry
a	width of peripheral parts of a specimen
R	radius of a hole
$\dot{u}_0$	rate of the crosshead movement
v_b	rate of the strain band propagation
k_b	coefficient of the strain inhomogeneity due to the Chernov-Lüder's behavior
R_{LS}	stiffness of a loading system
R_M	stiffness of a testing machine
R_c	stiffness of the additional deformable part of a specimen (the control part)
E	elasticity modulus